의학박사 학위논문

고산소 유도 하 R_1의 변화: 급성 뇌졸중에서 비가역적 뇌 손상의 자기공명영상 바이오마커

Hyperoxia-induced ΔR_1: MRI biomarker of irreversible ischemic damage in acute stroke

울 산 대 학 교 대 학 원
의 학 과
박 계 진

고산소 유도 하 R_1의 변화: 급성 뇌졸중에서 비가역적 뇌 손상의 자기공명영상 바이오마커

지 도 교 수　　김　정　곤

이 논문을 의학박사 학위 논문으로 제출함

2020 년 08 월

울 산 대 학 교 대 학 원
의　　학　　과
박 계 진

박계진의 의학박사학위 논문을 인준함

심사위원 김 호 성 인

심사위원 김 정 곤 인

심사위원 이 승 수 인

심사위원 김 경 원 인

심사위원 조 경 구 인

울 산 대 학 교 대 학 원

2020 년 08 월

영문요약

Purpose: Accurate and reliable measurement of irreversibly damaged area is an important diagnostic task in acute stroke, particularly for helping development of neuroprotective treatment. This study was performed to validate hyperoxia-induced ΔR_1 ($hyperO_2\Delta R_1$) as a useful imaging biomarker for identifying irreversible ischemic damage in stroke.

Materials and Methods: In cross-sectional experiment (12 rats, transient occlusion of middle-cerebral artery), $hyperO_2\Delta R_1$, apparent diffusion coefficient (ADC), ^{18}F-fluorodeoxyglucose uptake on positron emission tomography, cerebral blood flow and cerebral blood volumes were measured 2.5, 4.5, and 6.5 hours after stroke initiation. They were compared among infarct area, non-infarct ischemia and non-ischemic area on the criteria of histology and ADC. The levels of $hyperO_2\Delta R_1$ and ADC were voxel-wisely measured from the infarct core to the non-ischemic area. In longitudinal experiment (n=9), time-dependent changes of $hyperO_2\Delta R_1$ and ADC were analyzed at 3, 6, and 24 hours after initiation of transient stroke.

Results: In cross sectional study, $hyperO_2\Delta R_1$ increased exclusively in infarct area at all time points. In contrast, ADC gradually decreased from non-ischemic to infarct areas, and the other parameters did not show consistent patterns. $HyperO_2\Delta R_1$ showed a sharp decline from the core to the border of infarct areas and a plateaued level in non-infarct areas. Most voxels in infarct area showed hyperO2ΔR1 > 0.04 s-1. There was no noticeable difference of ADC at the border between infarct and non-infarct areas. In longitudinal study, $hyperO_2\Delta R_1$ was not reverted to normal level once having

gone higher than 0.04 s-1, and the area with hyper$O_2\Delta R_1$ higher than 0.04 s-1 continuously increased over time. ADC in infarct area showed inconsistent temporal changes in each rat.

Conclusion: Hyper$O_2\Delta R_1$ can be used as an accurate and reliable biomarker for identifying irreversible ischemic damage in stroke.

차 례

그림목차

서론

Currently, early restoration of blood flow to non-infarct ischemic area is the optimal treatment option to rescue brain tissue at risk of irreversible damage following acute stroke. However, a considerable number of stroke patients suffer from neurological deterioration after successful vascular recanalization, even without hemorrhagic transformation [1]. These undesirable results imply that progressive neuronal damage still occurs after successful reperfusion of salvageable tissue. Therefore, efficient neuroprotection is necessary to inhibit the catastrophic process that leads to irreversible ischemic damage [2].

Despite the high demand for neuroprotection in stroke, no FDA-approved treatment method is yet available. With this being the situation, the use of relevant biomarkers to accurately monitor the effect of neuroprotective treatment has been drawing attention as an important strategy to improve the success rate in translational research [3]. In particular, tracking whether the area undergoing irreversible damage increases over time or not will be useful to assess the effect of neuroprotection. Therefore, with the advantage of allowing repeated and quantitative data acquisitions in both preclinical and clinical settings, imaging parameters to distinguish irreversible from reversible damage are promising biomarker candidates in the development of neuroprotective treatments.

Although a number of imaging techniques have been used to identify reversible and irreversible damage in acute stroke, they present limitations for tracing the fate of ischemic tissue after sufficient restoration of perfusion. The apparent diffusion coefficient (ADC) calculated from diffusion-weighted imaging (DWI) is often renormalized during the aggravation of ischemic injury after recanalization [4, 5]. Blood oxygen-level dependent imaging to measure tissue oxygenation status is challenged by its vulnerability to factors other than oxygen level *per se* (i.e., the concentration of deoxyhemoglobin), and by the complexity in converting its signal to oxygen concentration [6]. Although positron emission tomography (PET) can provide crucial information on cerebral metabolism, it is not suitable for repeated examinations because of the radiation hazard and the low clinical availability of stroke-specific radiotracers such as $^{15}O_2$, $H_2{}^{15}O$, and ^{11}C-flumazenil [7-9].

Hyperoxia-induced ΔR_1 (hyper$O_2\Delta R_1$) has been acknowledged as a feasible magnetic resonance imaging (MRI) biomarker for measuring the tissue oxygen level [6, 10, 11].

Theoretically, this parameter is based on the oxygen-driven acceleration of longitudinal relaxation (quantified by increased R_1): the difference in R_1 between hyperoxic and normoxic breathing (i.e., hyper$O_2\Delta R_1$) indicates the amount of oxygen accumulation during hyperoxic respiration, and therefore demonstrates the status of oxygen delivery and the consumption by tissue. Recently, Suh et al [11] showed that hyper$O_2\Delta R_1$ significantly increased in infarct areas, and a criterion of hyper$O_2\Delta R_1$ (0.05 s^{-1}) dichotomized the distribution patterns of cell swelling, vasogenic edema, and glucose metabolism in 24 hour (H) transient stroke models. From these results, the authors suggested that the tissue oxygenation status quantified by hyper$O_2\Delta R_1$ can classify ischemic damage into reversible and irreversible stages in acute stroke.

Under the concept that accurate measurement of irreversibly damaged areas provides critical information about the trajectory of post-reperfusion stroke evolution, we designed this study to validate the potential of hyper$O_2\Delta R_1$ to identify irreversible damage in a transient-stroke rat model. We performed a cross-sectional study acquiring imaging at various time points after the onset of transient stroke to evaluate whether hyper$O_2\Delta R_1$ could accurately indicate areas with histological cell death. Thereafter, in a longitudinal study, we attempted to verify whether hyper$O_2\Delta R_1$ could indicate the irreversibility of ischemic damage and traced the change in hyper$O_2\Delta R_1$ after restoration of perfusion. On the basis of this systematic validation, we finally discuss the value of hyper$O_2\Delta R_1$ for monitoring the effectiveness of neuroprotective treatments for inhibiting progressive ischemic damage under restored perfusion in acute stroke.

연구재료 및 방법

All experimental protocols including the animal care and experimental procedures in this study were approved by the Institutional Animal Care and Use Committee of X.X. (blinded for peer review). Twenty-one adult male Wistar rats (weight, 280 to 300 g) were randomly allocated to cross-sectional (n = 12) or longitudinal (n = 9) experiments.

The study design is graphically summarized in Fig. 1.

Fig. 1.

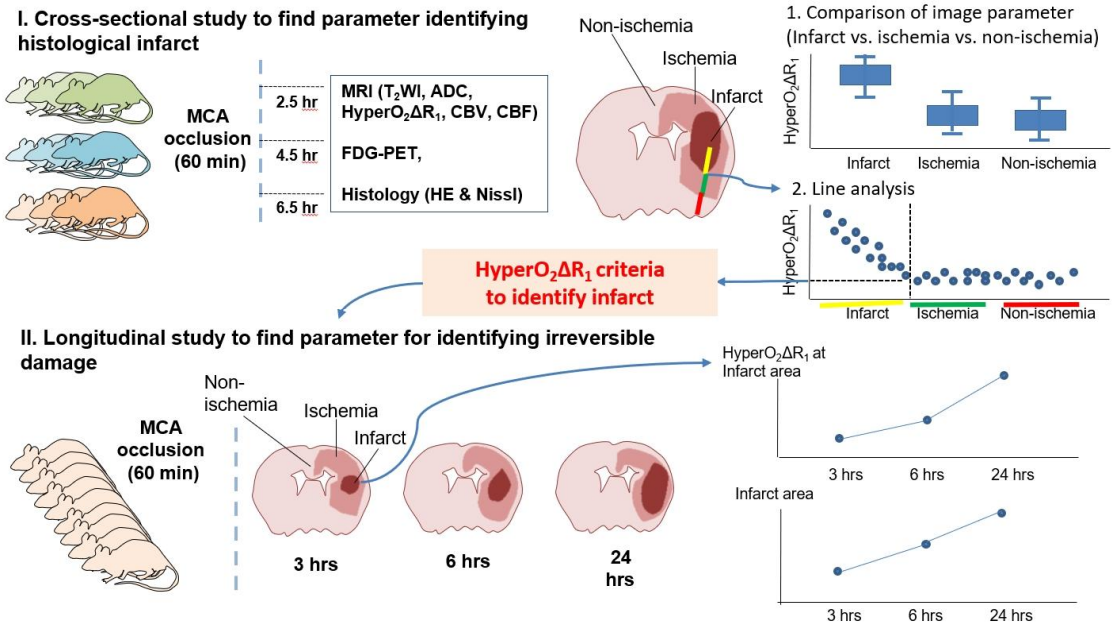

A graphical illustration of the procedures performed in this study. We conducted a cross-sectional study and a longitudinal study to determine optimal imaging biomarker after transient middle cerebral artery (MCA) occlusion in rat models. In the cross-sectional study, diffusion-weighted image and apparent diffusion coefficient map, hyper$O_2\Delta R_1$, cerebral blood flow, and cerebral blood volume on MRI and ^{18}F-FDG PET image were obtained across three time points (2.5, 4.5, and 6.5 hours after MCA occlusion), and values from those image parameters were compared among infarct, non-infarct ischemia, and non-ischemic areas. Consequently, we performed voxel-wise analysis from infarct core to non-ischemic area to identify the cut-off value to dichotomize infarct and ischemic area, and to correlate these area with histologic infarct area. In the longitudinal study, serial evaluation of apparent diffusion coefficient map and hyper$O_2\Delta R_1$ at 3, 6, and 24 hours after transient MCA occlusion was performed to evaluate temporal changes of infarct and ischemia, and to assess the irreversibility of MRI-defined infarct and ischemic area.

Transient Stroke Model

The rats were anaesthetized with 1.5% isoflurane in 70% N_2O/30% O_2 (flow rate, 1.0 l/min), and the right middle cerebral artery (MCA) was then occluded using the intraluminal filament technique, as previously described [12]. In brief, the common carotid artery and the proximal pterygopalatine artery were ligated using 4-0 silk suture. Thereafter, the superior thyroid and occipital branches of the external carotid artery were transected. Finally, a silicon rubber-coated 5-0 nylon monofilament (tip diameter, 0.31 ± 0.02 mm) was advanced 17 to 18 mm to the bifurcation along the internal carotid artery to occlude the MCA. After 60 min of MCA occlusion, the filament was carefully withdrawn to induce vascular re-canalization.

MRI, ^{18}F-FDG PET and histology parameters

Detailed information about the imaging sequence and measurement method of imaging parameters is presented in Table 1.

Table 1. The MR Imaging parameters

	T2-weighted imaging	**Diffusion-weighted imaging**	**Dynamic susceptibility contrast-enhanced imaging**	**R_1 map**
Sequence	Fast-spin echo sequence	Spin-echo EPI sequence	Gradient-echo EPI sequence	Relaxation-enhancement with variable repetition time sequence
TR/TE (ms)	4000/33	3000/18.7	1000/16	TR = 600, 900, 1500, 2500, 4000, and 7000; TE = 12.15
Other parameters	Rare factor = 8	*b* value (s/mm^2) = 0 and 800	Flip angle = 35°	Rare factor = 4
Field of view	28 x 28 mm	28 x 28 mm	28 x 28 mm	28 x 28 mm
Matrix size	96 x 96	96 x 96	96 x 96	64 x 64
Slice number	16	16	16	16
Slice thickness	1 mm	1 mm	1 mm	1 mm

Note.– EPI = echo planar imaging

MRI data were acquired using a 7.0 T Bruker pre-clinical MRI scanner (PharmaScan 70/16, Brucker BioSpin GmbH, Germany). Rats were positioned on a custom-made cradle and anesthetized with 1.5% to 2.0% isoflurane inhalation through a mask. A body temperature of 37°C was maintained using a temperature-controlled water blanket. The tail vein and femoral artery were cannulated with polyethylene catheters for MR contrast agent injection and blood sampling, respectively. MRI data included T2-weighted image (T_2WI), ADC images from DWI, and hyper$O_2\Delta R_1$ from R_1 mapping, and cerebral blood flow (CBF) and volume (CBV) from dynamic susceptibility contrast imaging, respectively.

^{18}F-FDG PET was obtained before MRI using nanoScanPET/MRI system (1T, Mediso, Hungary). Continuing to keep the rat warm, 6.5±1.0 MBq in 0.2 mL of FDG was administered via the tail vein under anesthesia (1.5% isoflurane in 100% O_2 gas). Static PET images were acquired for 20 min in a 1-5 coincident in a single field of view. PET images were reconstructed by Tera-Tomo 3D in full detector mode. Three-dimensional volume of interest analysis of the reconstructed images was performed using the InterView Fusion software package (Mediso, Hungary) and applying standard uptake value (SUV) analysis.

Light microscopy histologic examination was performed on mid-coronal sections of brain. Each brain section was stained with hematoxylin and eosin (H&E) and 0.25% cresyl violet for Nissl staining.

Image parameters were quantified using the Analysis of Functional NeuroImages (AFNI, National Institute of Health, Bethesda, MD, USA) program and ImageJ (National Institute of Health). Using the T_2WI as a reference frame, all parameter maps were co-registered and interpolated to achieve the same voxel geometry. For image-histology correlation, the slices of MRI and PET were selected and registered to corresponding digitized histological map.

Cross-sectional experiment

MRI and PET were performed at three time points of 2.5 H, 4.5 H, and 6.5 H following the initiation of transient stroke. Immediately after the imaging experiments, histological examinations were performed. We chose animals showing apparent infarction on histological map, and four rats were finally included for image analysis at each time point,

respectively.

The ipsilateral hemisphere was categorized into three areas based on the conjunction of incorporated histological and ADC information. Histological findings were used to determine the viability status of given cells. Cells were identified as being dead by cell body shrinkage, darkly stained pyknotic nuclei, and intensely-stained red eosinophilic cytoplasms in H&E staining as well as by a loss of Nissl substance in Nissl staining [13, 14]. Ipsilateral-to-contralateral ratio (ICR) of ADC less than 0.95 indicated ischemic cell damage as described in previous studies [11]. These criteria of cell death or damage then classified the ipsilateral hemisphere into three areas: infarct area (cell death), non-infarct ischemic area (cell damage without cell death), and non-ischemic area (no cell death or damage). Image parameters were compared among regions-of-interest (ROIs) drawn in the three areas.

With the mean values measured from ROI study, the boundary between infarction and non-infarction could not be clearly identified. Thus, to achieve a cut-off value to enhance the precision in delineating the border between the two areas, we performed a voxel-scaled continuous measurement of hyper$O_2\Delta R_1$ and ADC. In each rat, we drew a line from the infarct center to the periventricular non-ischemic region on images co-registered to the histologic map. Every line was drawn to cross the three areas proportionally identical: 60% of the total length of each line crossed the infarct area; 20% crossed the non-infarct ischemic area; and the remaining 20% crossed non-ischemic area. Then the value of hyper$O_2\Delta R_1$ and ADC in the voxels along the line were measured. In addition, the correlation was performed between the image parameters measured on the lines.

Finally, to validate whether the hyper$O_2\Delta R_1$ locate the infarct area, we assessed the spatial correlation between the hyper$O_2\Delta R_1$ and histological feature. The area of infarction indicated by hyper$O_2\Delta R_1$ was measured and then its ratio in the area of ipsilateral hemisphere was calculated. On the histological map, the area ratio of cell death lesion in the ipsilateral hemisphere was also estimated. Thereafter, the correlation between the two ratios was estimated.

Longitudinal experiment

The classification of ischemic injury at a certain time point in cross-sectional experiment does not necessarily inform the possibility of reversibility or irreversibility of affected brain. Moreover, as the ischemic burden may be inconsistent in terms of the velocity of progression to infarction, the comparison of image parameters across the time points is limited. Thus, we performed a longitudinal study to measure time-dependent changes of hyper$O_2\Delta R_1$ to demonstrate the trajectory of progression of a cerebral tissue after transient ischemic attack.

The hyper$O_2\Delta R_1$ and ADC were repeatedly measured at 3H, 6H and 24H, following stroke onset, and histological examinations were performed promptly after the 24-hour imaging study. The correlation between the hyper$O_2\Delta R_1$ and histology at 24 H was evaluated to validate the ability of hyper$O_2\Delta R_1$ to locate the infarct area throughout the entire stage of acute stroke.

On MRI obtained at 24H, the ipsilateral hemisphere was divided into infarct, non-infarct ischemic and non-ischemic areas by hyper$O_2\Delta R_1$ and ADC criteria by referring to the results in cross-sectional experiment. Thereafter, the status of each area at 3H and 6H was re-classified by the same criteria. For example, the infarct area on 24H MRI was subdivided into infarct, non-infarct ischemic and non-ischemic areas at 3H and 6H.

When the infarct was noted at 3H or 6H according to the criteria of hyper$O_2\Delta R_1$, the time-dependent change of hyper$O_2\Delta R_1$ in the initial infarct area was analyzed for evaluating the ability of hyper$O_2\Delta R_1$ to indicate the irreversible damage. The change of ADC was also analyzed.

Statistical Analysis

The ANOVA test was used to compare each value among the three areas. Linear regression analysis and Spearman correlation was used to evaluate the correlations between oxygen induced ΔR_1 and ADC, CBV, CBF, and ^{18}F-FDG uptake. A P value of < 0.05 was considered statistically significant.

결과

Cross-sectional Study

Increase in hyper$O_2\Delta R_1$ exclusively in the infarct area

Fig. 2 shows the values of each of the imaging parameters measured in the infarct area, non-infarct ischemic area, and non-ischemic area at the three time points. In comparison with the other parameters, hyper$O_2\Delta R_1$ showed a distinctive pattern in terms of discrimination of the infarct area, with increased values occurring exclusively in the infarct area ($P \leq 0.015$ compared with non-infarct ischemic and non-ischemic areas). This pattern was consistently observed at all three time points. By contrast, the ADC values demonstrated a pattern of stepwise decrease from the non-ischemic to infarct areas at all time points ($P=0.145$ at 2.5 H; $P \leq 0.007$ at 4.5 and 6.5 H). These results suggest that hyper$O_2\Delta R_1$ may be indicative of cell viability, and that the ADC may provide information on the degree of ischemic severity.

^{18}F-FDG uptake, CBF, and CBV did not show consistent differences between the three areas across the three time points. ^{18}F-FDG uptake was higher in the infarct area than in the other areas at 2.5 H, but this finding was not observed at 4.5 and 6.5 H. Likewise, a difference in CBF was observed only at the time point of 2.5 H ($P=0.072$), when the CBF value was slightly lower in the infarct area than in the others. CBV did not show any distinctive patterns of note across the time points and areas. The lack of significant between-area differences in the CBF and CBV levels at 4.5 and 6.5 H indicated that the blood supply was restored and evenly distributed across all areas after the transient occlusion of the MCA. Given inconsistent patterns or differences across the time points, the three parameters of ^{18}F-FDG, CBF, and CBV were considered to be inadequate for use as reproducible biomarkers for assessment of the degree of ischemic injury.

Fig. 2. Imaging biomarker values according to infarct or ischemic areas.

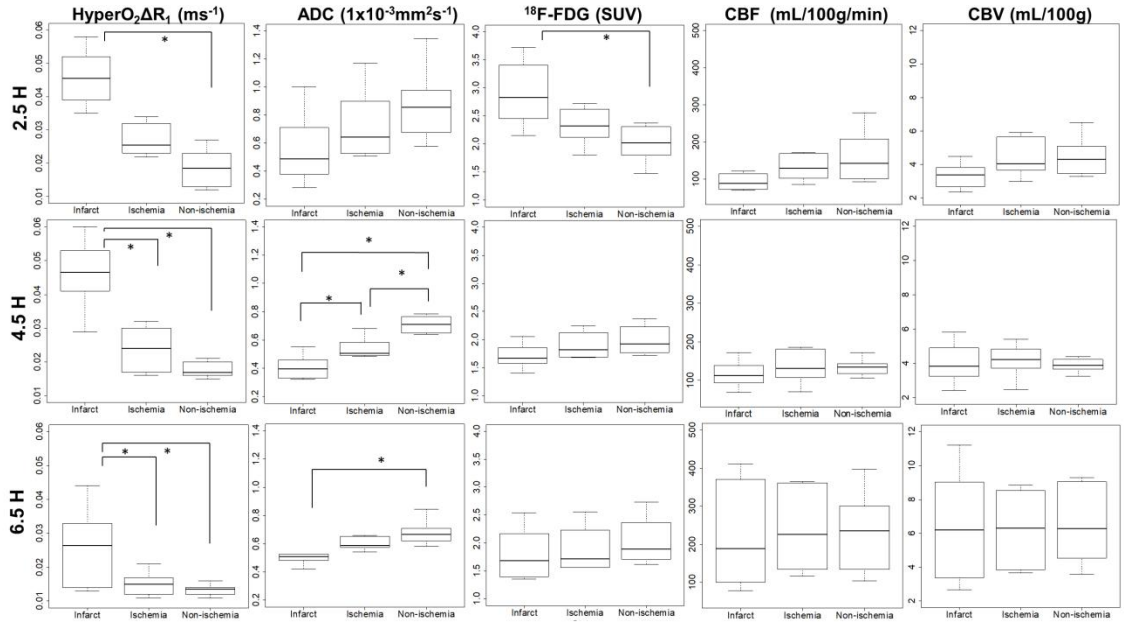

Imaging biomarker values according to infarct, ischemic, and non-ischemic areas at three time points after transient middle cerebral artery occlusion in the cross-sectional study. Box-and-whisker plots show the values of hyper$O_2\Delta R_1$, ADC, ^{18}F-FDG uptake, CBF, and CBV in three areas of different degrees of infarct and ischemic change. Hyper$O_2\Delta R_1$ shows an increase in values exclusively in the infarct area. This finding was consistent over the three time points. ADC values demonstrated a significant difference between the infarct and ischemic area, as well as between the ischemic and non-ischemic area at 4.5 and 6.5 H. ^{18}F-FDG uptake, CBF, and CBV demonstrated no differences in values across the three areas at the time points of 4.5 and 6.5 H, whereas a higher standardized uptake value and lower CBF value was transiently seen in the infarct area at 2.5 H. The asterisks indicate the significant differences between groups.

Voxel-wise analysis of hyper$O_2$$\Delta R_1$ and ADC

Based on the ROI experiments, hyper$O_2$$\Delta R_1$ and ADC were chosen as the imaging parameters worthy of further investigation for their ability to discriminate areas of irreversible ischemic damage from areas of reversible damage.

Hyper$O_2$$\Delta R_1$ and ADC showed different distributions. Hyper$O_2$$\Delta R_1$ showed a sharp decline in the voxel values moving from the core to the border of the infarct areas, whereas there was no change within the non-infarct areas (Fig. 3a). Hyper$O_2$$\Delta R_1$ was greater than 0.04 s^{-1} in most of the voxels included in the infarct area, and less than 0.04 s^{-1} in the voxels in the non-infarct areas. There was no notable difference in hyper$O_2$$\Delta R_1$ between the non-infarct ischemic and non-ischemic areas. However, a gradual increase in ADC values from the infarct core to the periphery was observed, without a pronounced difference at the border between the infarct and non-infarct ischemic areas (Fig. 3b). Thus, it was difficult to assign a clear ADC cut-off value that would allow clear definition of the border between the infarct and non-infarct areas.

The correlation between hyper$O_2$$\Delta R_1$ and ADC showed a dichotomized pattern, as shown in Figure 3c. In the voxels with hyper$O_2$$\Delta R_1$ less than 0.04 s^{-1}, most of which were identified in the non-infarcted and non-ischemic areas, hyper$O_2$$\Delta R_1$ and ADC showed a strong negative correlation. By contrast, the voxels with hyper$O_2$$\Delta R_1$ greater than 0.04 s^{-1}, which were observed mostly in the infarct area, showed plateaued ADC values, regardless of the hyper$O_2$$\Delta R_1$ values measured. This dichotomized distribution was consistently observed at all time points after stroke onset. The negative correlation between the two parameters demonstrated that cell edema gradually progressed because of continual energy failure, while the plateaued correlation reflects the fact that brain tissue with hyper$O_2$$\Delta R_1$ above 0.04 s^{-1} was maintained under the highest degree of cellular edema or restricted cytoplasmic movement. Therefore, we presume that a hyper$O_2$$\Delta R_1$ of 0.04 s^{-1} could potentially indicate that ischemic cells have reached a state of complete membrane failure in acute stroke.

Fig. 3. Continuous voxel-wise analysis of hyper$O_2\Delta R_1$ and ADC values

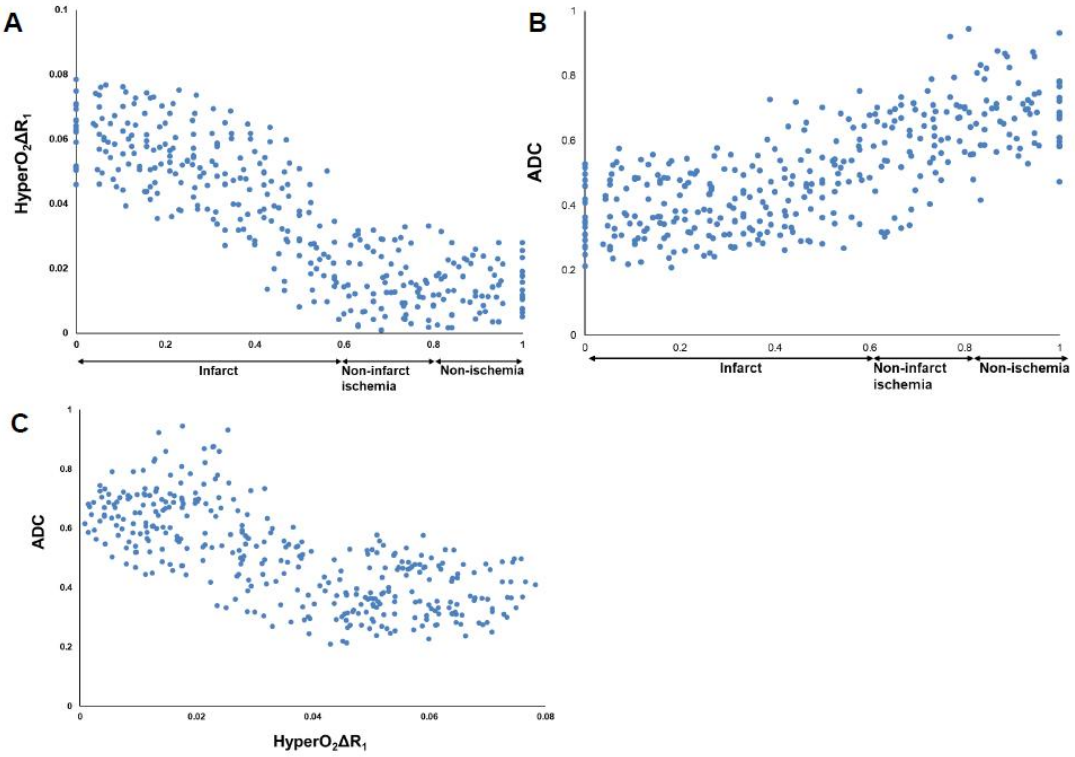

Continuous voxel-wise analysis of hyper$O_2\Delta R_1$ and ADC values from the center of the infarct to the non-ischemic area. **a.** Scatterplot demonstrates a clear transition in hyper$O_2\Delta R_1$ values at the border of the infarct and non-infarct ischemia at the cutoff of 0.4 s^{-1}. **b.** ADC values monotonically increase from the infarct core to the non-ischemic area, with no clear boundary being seen between areas. **c.** A scatterplot demonstrates the negative correlation between hyper$O_2\Delta R_1$ and ADC values below the hyper$O_2\Delta R_1$ cutoff of 0.04 s^{-1}, and a plateaued distribution of ADC values above the value of 0.04 s^{-1}.

Correspondence between the areas with hyper$O_2$$\Delta R_1$ higher than 0.04 s^{-1} and the histologically identified infarct areas

The area of hyper$O_2\Delta R_1$ higher than 0.04 s^{-1} showed a strong positive correlation with that of histological cell death ($r = 0.823$; $P < 0.001$) (Fig 4.). On visual inspection, the area of hyper$O_2\Delta R_1$ higher than 0.04 s^{-1} spatially corresponded with the histologically determined cell-death areas. Consequently, hyper$O_2\Delta R_1$ was regarded as an accurate indicator of the location of the histological infarct area.

Fig. 4. Correlation between histologic infarct and hyper$O_2\Delta R_1$ greater than 0.04 s^{-1}

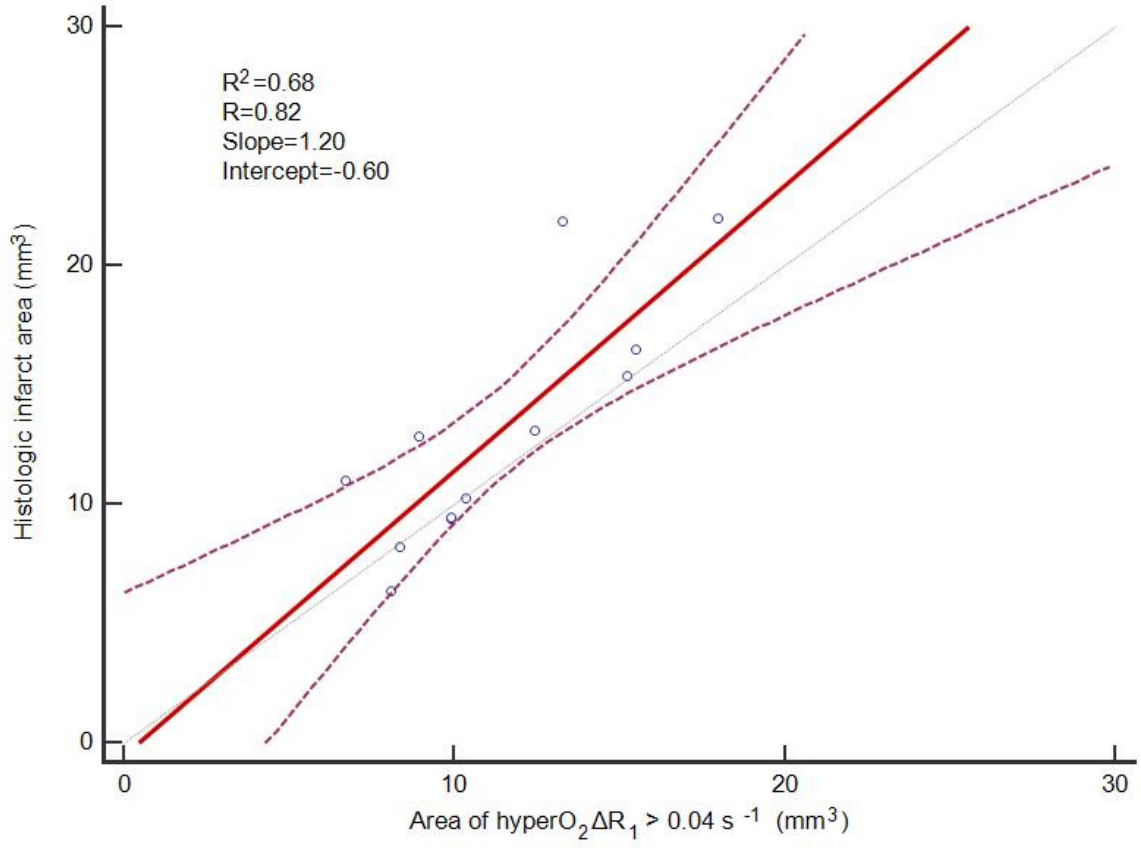

Correlation between the histologically-defined infarct area and the area with hyper$O_2\Delta R_1$ greater than 0.04 s^{-1}. A strong positive correlation between the two areas was observed (rho = 0.82, R^2=0.68, Slope=1.20).

Longitudinal measurement of hyper$O_2\Delta R_1$ and ADC in the transient stroke model

By referring to the results of cross-sectional experiment, the ipsilateral hemisphere was classified into infarct, non-infarct ischemic, and non-ischemic areas using the following criteria: infarct area = hyper$O_2\Delta R_1 \geq 0.04$ s^{-1}; non-infarct ischemia = hyper$O_2\Delta R_1 < 0.04$ s^{-1} and an ADC ICR of < 0.95; and non-ischemic areas = hyper$O_2\Delta R_1 < 0.04$ s^{-1} and an ADC ICR > 0.95.

Fig. 5. shows the proportions of infarct, non-infarct ischemic, and non-ischemic areas in the ipsilateral hemisphere at 3, 6, and 24 H after stroke onset. All rats demonstrated expansion of the infarct area over time, while the proportional area of non-ischemia decreased over time in all rats. These data demonstrate that infarction progressed after vascular recanalization, and that a normal ADC level in the early stage of stroke did not necessarily indicate exemption from ischemic damage.

Although expansion of infarction was consistently observed in all rats, the onset time of the infarction varied across the rats, being initially observed at 3, 6, or 24 H. The initial occurrence time of infarction did not necessarily provide information on the infarct volume at 24 H. This result implies that infarction may occur at any stage of acute stroke.

Fig. 5. The proportions of infarct, non-infarct ischemic, and non-ischemic areas at 3, 6, and 24 hours after stroke onset

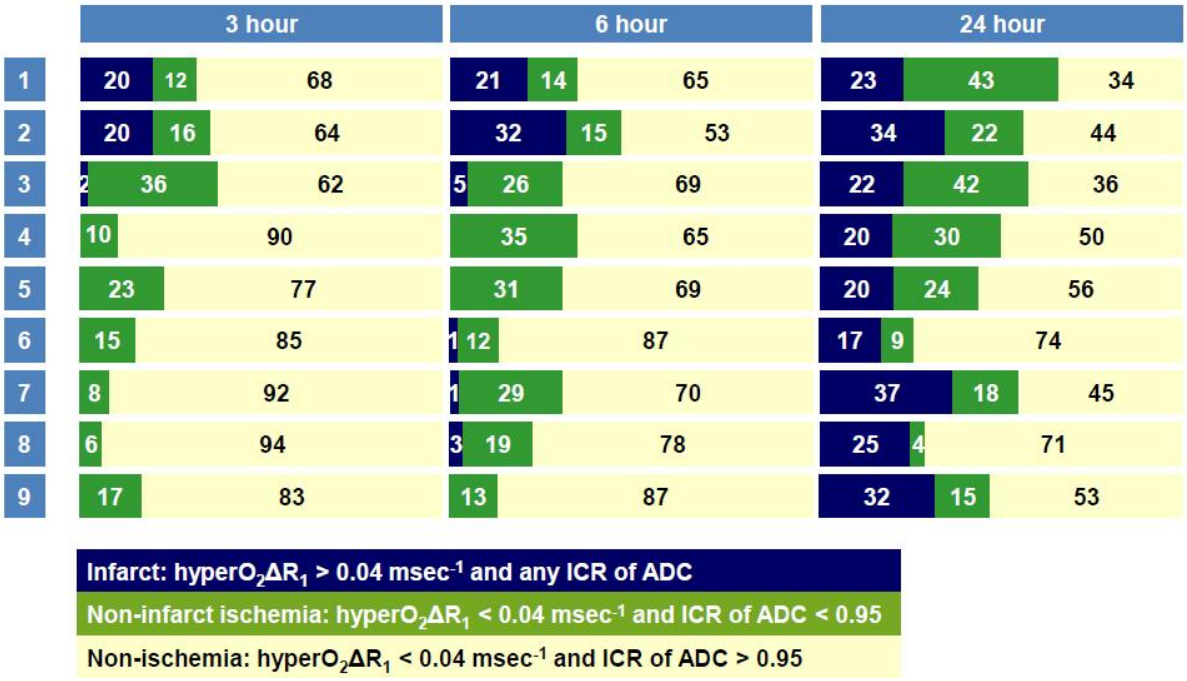

The proportions of infarct, non-infarct ischemic, and non-ischemic areas at 3, 6, and 24 hours after stroke onset in nine rats. Infarct areas irreversibly increased over time, while early-stage non-ischemic areas progressed to infarct and non-infarct ischemic areas.

Irreversibility of the area with HyperO_2ΔR_1 higher than 0.04 s^{-1}

In six rats, the area with hyperO_2ΔR_1 values higher than 0.04 s^{-1} at 3 or 6 H continued to increase until 24 H, demonstrating progression of metabolic dysfunction. Moreover, no voxel within these areas demonstrated a decrease in hyperO_2ΔR_1 to a level below 0.04 s^{-1} over the time (Fig. 6a). Along with the finding of an increasing area with hyperO_2ΔR_1 > 0.04 s^{-1} over time, this unidirectional temporal change in hyperO_2ΔR_1 supports the use of hyperO_2ΔR_1 values higher than 0.04 s^{-1} as an indicator of irreversible damage.

Inconsistent temporal change in ADC within the infarct area

Temporal changes in ADC were assessed in each rat in the longitudinal study. The ADC values in the infarct area on the 24 H MRI showed inconsistent changes between 3 and 24 H in each rat (Fig. 6b). This finding indicates that ADC is not suitable as a parameter to assess the status of ischemic damage in infarct areas.

Fig. 6.

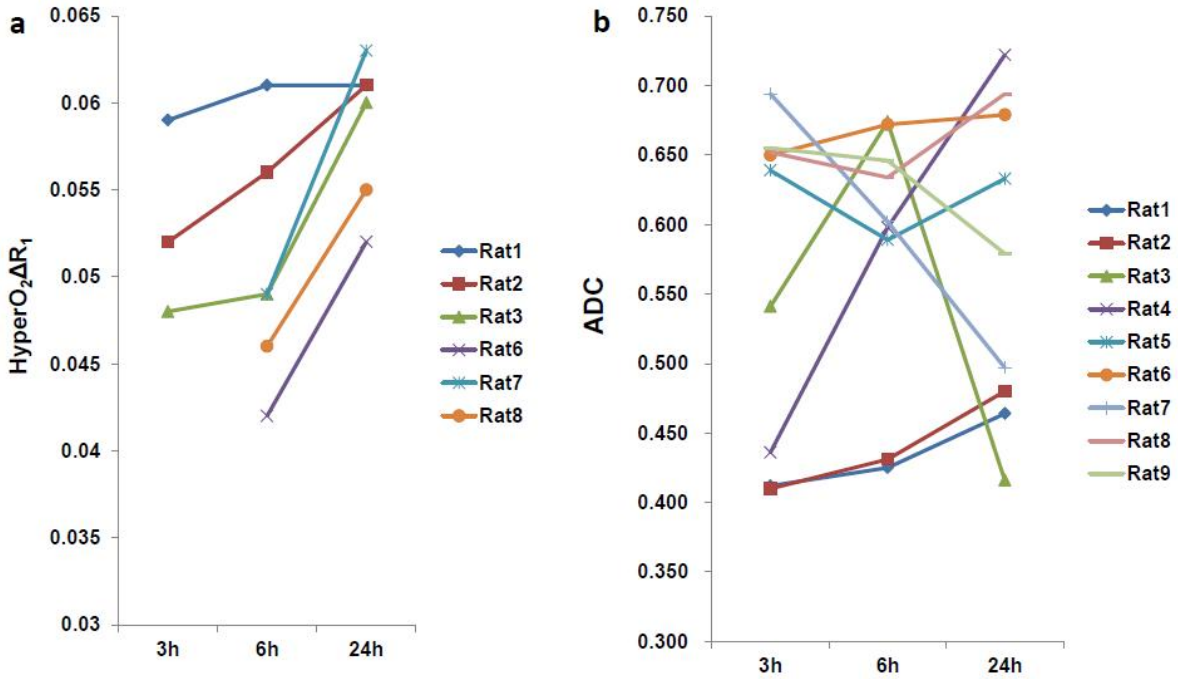

Progression and irreversibility of the infarct area identified by hyper$O_2\Delta R_1 > 0.04$ s^{-1}. **a.** In six rats that demonstrated hyper$O_2\Delta R_1 > 0.04$ s^{-1} at 3 hours, the values of hyper$O_2\Delta R_1$ increased. **b.** The areas defined as infarct on 24 hour MRI showed inconsistent ADC values over the three time points.

Temporal change in the ipsilateral hemisphere under ischemia

Fig. 7. shows the proportions of infarct, non-infarct ischemia, and non-ischemia areas at 3 and 6 H within the areas of infarct, non-infarct ischemia, and non-ischemia defined at 24 H. In all rats, a significant portion of the area identified as infarct at 24 H was previously in the state of non-infarct ischemia or non-ischemia at 3 and 6 H. Similarly, a meaningful portion of the area identified as non-infarct ischemia at 24 H was non-ischemic at 3 and 6 H. These data suggest that progressive neuronal damage occurs after vascular recanalization, and that a normal ADC level does not necessarily indicate immunity from ischemic damage in the aftermath of the onset of acute stroke.

Fig. 7.

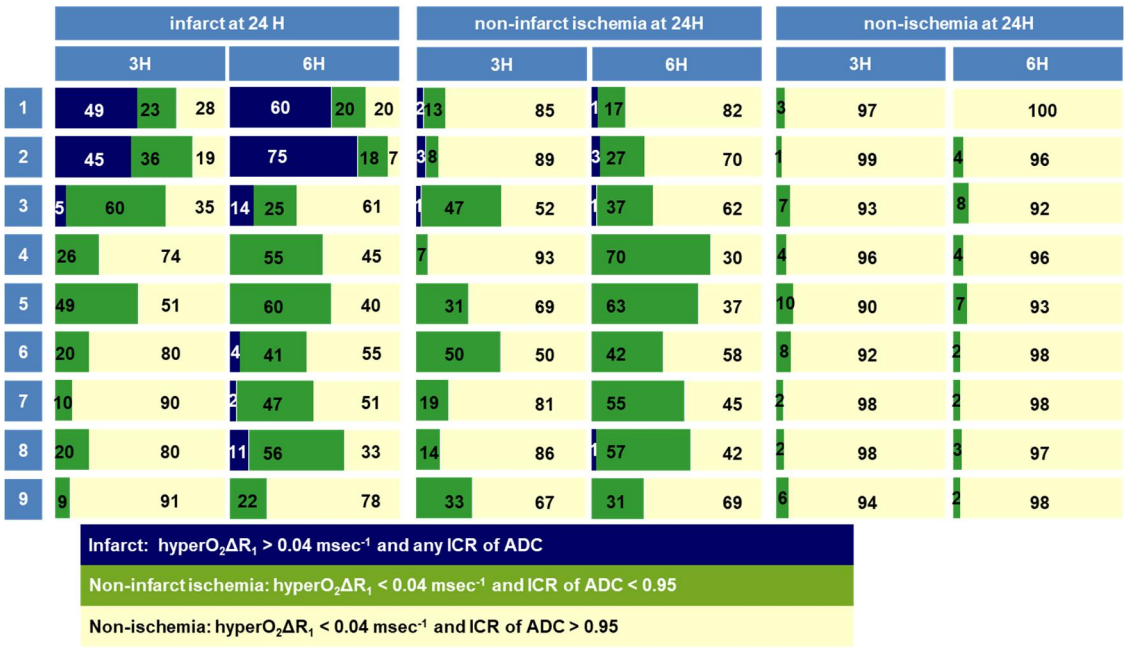

Proportions of infarct, non-infarct ischemia, and non-ischemia at 3 and 6 hours after stroke onset within the areas defined as infarct, non-infarct ischemia, and non-ischemia at 24 hours. Significant proportions of the infarct area identified at 24 hours were identified as non-infarct ischemia and non-ischemia at the previous time points, suggesting progressive neuronal loss after vascular recanalization. By contrast, some portions showing ischemic changes at 3 and 6 hours had normalized at 24 hours.

고찰

In our cross-sectional experiment, hyper$O_2\Delta R_1$ showed an increase at various time points exclusively in the areas that showed histological cell death, displaying notable differences at the borders between cell-death areas and other areas. Our experiments subsequently showed that the area with hyper$O_2\Delta R_1$ higher than 0.04 s^{-1} was very similar to the area showing cell death on histological analysis. In the longitudinal experiment, hyper$O_2\Delta R_1$ did not revert to a normal level once it had gone above 0.04 s^{-1}, and the area with hyper$O_2\Delta R_1$ of 0.04 s^{-1} and above showed a continuous increase over the 24 H following stroke. The results of our cross-sectional and longitudinal experiments complement and support each other to demonstrate that hyper$O_2\Delta R_1$ higher than 0.04 s^{-1} is a reliable indicator of irreversible ischemic damage in stroke.

The hyper$O_2\Delta R_1$ value is determined by the balance between oxygen delivery and consumption in tissue. When the blood supply is restored to ischemic brain (i.e., ischemia/reperfusion injury) and the partial or full normalization of vascular oxygen delivery occurs, cellular oxygen utilization for energy production remains hypoactivated. This condition leads to an accumulation of unconsumed oxygen during hyperoxic respiration, which consequently increases the hyper$O_2\Delta R_1$ (i.e., the difference in R_1 between hyperoxic and normoxic respiration). Therefore, hyper$O_2\Delta R_1$ elevation in transient ischemic brain is an MRI phenotype reflecting impaired oxygen metabolism.

As mitochondria consume oxygen for energy production, the hyper$O_2\Delta R_1$ quantification of unconsumed oxygen indicates the degree of mitochondrial dysfunction. Studies show that various harmful processes in mitochondria, such as altered bioenergenetics, disorganized structural architecture, and aberrant biochemical dynamics, have a pivotal role in neuronal death in stroke [15]. Mitochondrial damage leads not only to depletion of energy production, but also to overproduction of reactive oxygen species. In addition to collapse of electrophysiological homeostasis due to a lack of energy, reactive oxygen species induce a number of pathological processes that cause neuronal death, such as caspase activation, the release of inflammatory mediators, and oxidative damage to the cell [16, 17]. Therefore, our criteria of 0.04 s^{-1} or higher hyper$O_2\Delta R_1$, which showed a close correlation between

histological cell death and failure of renormalization, indicate irreversible neuronal death triggered by mitochondrial dysfunction in stroke.

In our longitudinal study, extended irreversible ischemic damage ($hyperO_2\Delta R_1 \geq 0.04\ s^{-1}$) was observed, even after the restoration of perfusion (ICR of CBF ≥ 0.95). This suggests that successful intravenous thrombolysis or mechanical thrombectomy in patients with acute stroke may not prevent undesirable clinical outcomes [18]. Despite a high success rate of early vascular recanalization (higher than 80%), more than half of patients fail to acquire functional independence [1, 2].

A number of pharmacological agents have been developed for the neuroprotection of patients with stroke [19-21]. However, clinical trials of neuroprotective treatments have failed to translate preclinical effects into clinically meaningful outcomes [15]. Determination of the causes of the current barriers against the development of neuroprotective treatments has resulted in the demand for adequate biomarkers to bridge the gap between preclinical and clinical studies. At the same time, the adequacy of the biomarkers currently used for outcome evaluation has been put into question [22]. For example, parameters used in clinical assessment, such as the National Institute of Heath Stroke Scale, Barthel Index, and Rankin Scale, cannot be adequately applied to preclinical studies. This inadequacy is also true for imaging biomarkers, as their ability to test the effects of neuroprotective treatment has not been fully verified.

T2WI, DWI, and perfusion imaging have been widely used to measure areas with reversible or irreversible damage in both preclinical and clinical trials [23-25]. However, the origins of the signals on T2-weighted imaging (water content), DWI (diffusivity of water protons), and perfusion imaging (delivery of contrast material) do not provide information on cell viability, and accurate cut-off values to distinguish reversible and irreversible damage have not been identified for these MRI methods. Furthermore, perfusion imaging has a significant limitation in terms of reliability, as perfusion-related parameters vary according to the calculation algorithm and the location used to extract the arterial input function [26 27].

In response to these limitations, we attempted to systemically validate the relevance, accuracy, and reliability of $hyperO_2\Delta R_1$ for identifying regions with irreversible damage, and found the following; (a) Measurements at various time points showed the time-consistency

of hyper$O_2\Delta R_1$ for identifying irreversible damage. (b) Voxel-wise analysis allowed the establishment of criteria to delineate the border between infarct and non-infarct areas. (c) The areas with histological cell death and hyper$O_2\Delta R_1$ higher than 0.04 s^{-1} were found to be very similar to each other. (d) Longitudinal study showed a non-exceptional and continuous increase in hyper$O_2\Delta R_1$ over time in the cell death area. We suggest that these findings validate the efficacy and reliability of hyper$O_2\Delta R_1$ higher than 0.04 s^{-1} for assessing the effects of neuroprotective treatments.

The present study demonstrated that the ADC is not an adequate marker to identify irreversible ischemic damage; because of the gradual procession from non-ischemia to infarct, it was difficult to assign a cut-off ADC value to delineate the infarct area. Moreover, as noted in our longitudinal study, the ADC level in the infarct core alters because of various conditions other than cytotoxic edema, such as cellular lysis, hemorrhagic transformation, and early vasogenic edema [28]. Despite these limitations, as the ADC is particularly useful for assessing ischemic damage, we recommend the combined implementation of ADC and hyper$O_2\Delta R_1$ (decreased ADC and hyper$O_2\Delta R_1$ lower than 0.04 s^{-1}) to provide more accurate and reliable information for identifying non-infarct ischemia. Using these criteria, improvement from non-infarct ischemia to non-ischemia can be identified, as in the case of spontaneous improvement shown in this study.

To apply hyper$O_2\Delta R_1$ in clinical circumstances, it is necessary to address several potential challenges. First, it has been reported that long duration (usually > 60 minute) hyperbaric oxygen therapy presents a risk of harmful effects [29, 30]. That is, administration of 100% O_2 for several minutes during the measuring of R_1 value could result in oxygen toxicity. In regard to this concern, it would be fair to suggest that the application of hyper$O_2\Delta R_1$ involves no such risk, as hyperoxic normobaric respiration during the hyper$O_2\Delta R_1$ measurement takes a short period of time and is unlikely to produce any harmful effects. Nevertheless, to completely remove such a risk, a maximum measuring time to guarantee safety needs to be established. The inevitable extension of examination time because of our recommended acquisition of multiple parameters (hyper$O_2\Delta R_1$ in conjunction with ADC or CBF) is another important point of concern, as it is critical to minimize the scanning time for patients with acute stroke. In response to this potential drawback, we

propose the application of ultrafast scanning techniques. Using the Look-Locker technique, R_1 maps of the whole human brain can be acquired within 2 minutes, with a spatial resolution of $1.1 \times 1.1 \times 4$ mm^3 [31]. Another faster MRI sequence is the ultrafast low-angle RARE sequence, which has a temporal resolution allowing measurement of R_1 in the mouse brain within 6 s [32]. Moreover, as the R_1 relaxation time can be influenced by magnetic field strength, the cutoff of hyper$O_2\Delta R_1 > 0.04$ s^{-1} determined in our study under 9.4 T MRI could not be generally applied to 1.5 T or 3 T MRI. For example, the cutoff of 0.05 s^{-1} used in the previous study was determined under 4.7 T MRI, thus it needs further refinement before the application of clinical study.

결론

In summary, our cross-sectional experiment showed that hyper$O_2\Delta R_1$ higher than 0.04 s^{-1} delineated the histological cell death area on MRI. Our longitudinal experiment then validated the reliability of hyper$O_2\Delta R_1$ as an indicator of irreversible ischemic damage. In conjunction with other traditional MRI parameters, hyper$O_2\Delta R_1$ could help measure the severity of ischemic damage and monitor the effectiveness of neuroprotective treatment in acute stroke.

국문요약

서론: 급성 뇌졸중에서 허혈에 의한 뇌조직의 변화를 구분하고 비가역적인 조직 손상을 정량화 할 수 있는 영상의학적 바이오마커는 임상적 및 전임상적 연구에 있어 중요하다. 이에 새로운 자기공명영상 바이오마커인 고산소유도 하 R_1 의 변화 (hyperoxia-induced ΔR_1)가 비가역적인 뇌 조직손상을 구분할 수 있는지 알고자 하였다.

연구방법: 일시적 뇌허혈을 유발시킨 12 마리의 쥐 모델에서 다섯 가지의 영상검사 (hyperoxia-induced ΔR_1, 확산 강조영상 및 현성확산계수 [diffusion-weighted image and apparent diffusion coefficient, ADC], 양전자방출 단층촬영 [^{18}F-fluorodeoxyglucose uptake]과 대뇌혈류 (cerebral blood flow and cerebral blood volume)를 뇌 허혈 이후 2.5 시간, 4.5 시간, 및 6.5 시간 이후 시행하였다. 이들이 조직학적 경색, 허혈 및 비허혈 조직에서 어떠한 패턴을 보이는지 분석하였다. 또한 9 마리의 쥐 모델에서 각각 뇌졸중 발생 3 시간, 6 시간 및 24 시간에서 hyperoxia-induced ΔR_1 과 ADC 값의 변화 양상을 분석하여 이 바이오마커들의 시간에 따른 비가역성을 알고자 하였다.

결과: Hyperoxia-induced ΔR_1 은 조직학적 경색 부위에서 허혈 혹은 비허혈 조직에 비해 2.5 시간, 4.5 시간, 및 6.5 시간 모두에서 유의한 증가를 보였으며, 그에 반해 ADC 는 조직학적 경색 부위에서 낮은 값을 보이고 허혈과 비허혈 조직에서 점차 증가하는 양상을 보였다. 그러나 양전자방출 단층촬영이나 MRI 로 측정한 대뇌혈류는 이 세 조직 간의 유의한 차이를 보이지 않았다. 복셀 단위의 분석에서 hyperoxia-induced ΔR_1 은 조직학적 경색 부위에서 매우 높은 값을 보이나, 비경색 부위에서는 평평한 값을 보여, 경색과 비경색 부위 사이에서 급격한 변화를 보였다. Hyperoxia-induced ΔR_1 이 0.04 s^{-1} 보다 큰 영역은 조직학적 경색과 강한 상관관계를 보였다 (상관계수 = 0.823; $P < 0.001$). Hyperoxia-induced ΔR_1 이 0.04 보다 높은 영역은 뇌졸중 발생 이후 3 시간, 6 시간 및 24 시간에서 점차 값이 증가하고 영역이 넓어지는 비가역적인 변화를 보였다.

결론: Hyperoxia-induced ΔR_1 은 허혈성 뇌졸중에서 비가역적인 뇌조직 손상을 의미있게 구분할 수 있는 유용한 자기공명영상 바이오마커이며, 뇌졸중의 경과 및 치료반응을 평가하는데 그 유용성이 기대된다.

중심단어: 고산소 유도하 R_1의 변화; 허혈성 뇌졸중; 경색; 뇌조직; 바이오마커

참고문헌

1. Zhang YB, Su YY, He YB, Liu YF, Liu G, Fan LL. Early neurological deterioration after recanalization treatment in patients with acute ischemic stroke: A retrospective study. *Chinese medical journal*. 2018;131:137-143
2. Baron JC. Protecting the ischaemic penumbra as an adjunct to thrombectomy for acute stroke. *Nature reviews. Neurology*. 2018;14:325-337
3. Fisher M, Feuerstein G, Howells DW, Hurn PD, Kent TA, Savitz SI, et al. Update of the stroke therapy academic industry roundtable preclinical recommendations. *Stroke*. 2009;40:2244-2250
4. Li F, Liu K-F, Silva MD, Meng X, Gerriets T, Helmer KG, et al. Acute postischemic renormalization of the apparent diffusion coefficient of water is not associated with reversal of astrocytic swelling and neuronal shrinkage in rats. *American Journal of Neuroradiology*. 2002;23:180-188
5. Leigh R, Knutsson L, Zhou J, van Zijl PC. Imaging the physiological evolution of the ischemic penumbra in acute ischemic stroke. *J Cereb Blood Flow Metab*. 2018;38:1500-1516
6. Colliez F, Safronova MM, Magat J, Joudiou N, Peeters AP, Jordan BF, et al. Oxygen mapping within healthy and acutely infarcted brain tissue in humans using the nmr relaxation of lipids: A proof-of-concept translational study. *PloS one*. 2015;10:e0135248
7. Baron JC. How healthy is the acutely reperfused ischemic penumbra? *Cerebrovascular diseases (Basel, Switzerland)*. 2005;20 Suppl 2:25-31
8. Baron JC. Mapping the ischaemic penumbra with pet: Implications for acute stroke treatment. *Cerebrovasc Dis*. 1999;9:193-201
9. Kuge Y, Yokota C, Tagaya M, Hasegawa Y, Nishimura A, Kito G, et al. Serial changes in cerebral blood flow and flow-metabolism uncoupling in primates with acute thromboembolic stroke. *J Cereb Blood Flow Metab*. 2001;21:202-210
10. O'Connor JP, Boult JK, Jamin Y, Babur M, Finegan KG, Williams KJ, et al. Oxygen-enhanced mri accurately identifies, quantifies, and maps tumor hypoxia in preclinical

cancer models. *Cancer Res*. 2016;76:787-795

11. Suh JY, Cho G, Song Y, Woo DC, Choi YS, Ryu EK, et al. Hyperoxia-induced deltar1. *Stroke*. 2018;49:3012-3019
12. Longa EZ, Weinstein PR, Carlson S, Cummins R. Reversible middle cerebral artery occlusion without craniectomy in rats. *Stroke*. 1989;20:84-91
13. Zille M, Farr TD, Przesdzing I, Muller J, Sommer C, Dirnagl U, et al. Visualizing cell death in experimental focal cerebral ischemia: Promises, problems, and perspectives. *J Cereb Blood Flow Metab*. 2012;32:213-231
14. Li H, Zhang N, Lin H-Y, Yu Y, Cai Q-Y, Ma L, et al. Histological, cellular and behavioral assessments of stroke outcomes after photothrombosis-induced ischemia in adult mice. *BMC Neuroscience*. 2014;15:58
15. Liu F, Lu J, Manaenko A, Tang J, Hu Q. Mitochondria in ischemic stroke: New insight and implications. *Aging Dis*. 2018;9:924-937
16. Yang J-L, Mukda S, Chen S-D. Diverse roles of mitochondria in ischemic stroke. *Redox Biol*. 2018;16:263-275
17. Crack PJ, Taylor JM. Reactive oxygen species and the modulation of stroke. *Free radical biology & medicine*. 2005;38:1433-1444
18. Yang Q, Huang Q, Hu Z, Tang X. Potential neuroprotective treatment of stroke: Targeting excitotoxicity, oxidative stress, and inflammation. *Front Neurosci*. 2019;13:1036-1036
19. Narayanan SV, Dave KR, Saul I, Perez-Pinzon MA. Resveratrol preconditioning protects against cerebral ischemic injury via nuclear erythroid 2-related factor 2. *Stroke*. 2015;46:1626-1632
20. Peng C, Rao W, Zhang L, Wang K, Hui H, Wang L, et al. Mitofusin 2 ameliorates hypoxia-induced apoptosis via mitochondrial function and signaling pathways. *The international journal of biochemistry & cell biology*. 2015;69:29-40
21. Tucker D, Lu Y, Zhang Q. From mitochondrial function to neuroprotection-an emerging role for methylene blue. *Mol Neurobiol*. 2018;55:5137-5153
22. Kim SJ, Moon GJ, Bang OY. Biomarkers for stroke. *Journal of stroke*. 2013;15:27-37
23. Singhal AB, Benner T, Roccatagliata L, Koroshetz WJ, Schaefer PW, Lo EH, et al. A

pilot study of normobaric oxygen therapy in acute ischemic stroke. *Stroke*. 2005;36:797-802

24. Wintermark M, Albers GW, Broderick JP, Demchuk AM, Fiebach JB, Fiehler J, et al. Acute stroke imaging research roadmap ii. *Stroke*. 2013;44:2628-2639
25. Butcher KS, Parsons MW, Davis S, Donnan G. Pwi/dwi mismatch: Better definition required. *Stroke*. 2003;34:e215-216; author reply e215-216
26. Kidwell CS. Mri biomarkers in acute ischemic stroke: A conceptual framework and historical analysis. *Stroke*. 2013;44:570-578
27. Bateman M, Slater L-A, Leslie-Mazwi T, Simonsen CZ, Stuckey S, Chandra RV. Diffusion and perfusion mr imaging in acute stroke: Clinical utility and potential limitations for treatment selection. *Topics in Magnetic Resonance Imaging*. 2017;26:77-82
28. Pierpaoli C, Righini A, Linfante I, Tao-Cheng JH, Alger JR, Chiro GD. Histopathologic correlates of abnormal water diffusion in cerebral ischemia: Diffusion-weighted mr imaging and light and electron microscopic study. *Radiology*. 1993;189:439-448
29. Ding Z, Tong WC, Lu XX, Peng HP. Hyperbaric oxygen therapy in acute ischemic stroke: A review. *Interventional neurology*. 2014;2:201-211
30. Rusyniak DE, Kirk MA, May JD, Kao LW, Brizendine EJ, Welch JL, et al. Hyperbaric oxygen therapy in acute ischemic stroke: Results of the hyperbaric oxygen in acute ischemic stroke trial pilot study. *Stroke*. 2003;34:571-574
31. Jiang K, Zhu Y, Jia S, Wu Y, Liu X, Chung YC. Fast t1 mapping of the brain at high field using look-locker and fast imaging. *Magnetic resonance imaging*. 2017;36:49-55
32. Pastor G, Jimenez-Gonzalez M, Plaza-Garcia S, Beraza M, Reese T. Fast t1 and t2 mapping methods: The zoomed u-flare sequence compared with epi and snapshot-flash for abdominal imaging at 11.7 tesla. *Magma (New York, N.Y.)*. 2017;30:299-307